

This article was downloaded by:

On: 22 January 2011

Access details: *Access Details: Free Access*

Publisher *Taylor & Francis*

Informa Ltd Registered in England and Wales Registered Number: 1072954 Registered office: Mortimer House, 37-41 Mortimer Street, London W1T 3JH, UK



## The Journal of Adhesion

Publication details, including instructions for authors and subscription information:

<http://www.informaworld.com/smpp/title~content=t713453635>

### Utilization of Contact Resistance Measurements in the Investigation of the Metallic Adhesion of Iron

T. McNicholas<sup>a</sup>; D. V. Keller Jr.<sup>b</sup>

<sup>a</sup> Standard Oil Company of California, Richmond, California <sup>b</sup> Associate Professor of Metallurgy, Syracuse University, Syracuse, N.Y.

Online publication date: 05 November 2010

**To cite this Article** McNicholas, T. and Keller Jr., D. V.(1969) 'Utilization of Contact Resistance Measurements in the Investigation of the Metallic Adhesion of Iron', *The Journal of Adhesion*, 1: 3, 164 — 179

**To link to this Article:** DOI: 10.1080/00218466908078890

**URL:** <http://dx.doi.org/10.1080/00218466908078890>

PLEASE SCROLL DOWN FOR ARTICLE

Full terms and conditions of use: <http://www.informaworld.com/terms-and-conditions-of-access.pdf>

This article may be used for research, teaching and private study purposes. Any substantial or systematic reproduction, re-distribution, re-selling, loan or sub-licensing, systematic supply or distribution in any form to anyone is expressly forbidden.

The publisher does not give any warranty express or implied or make any representation that the contents will be complete or accurate or up to date. The accuracy of any instructions, formulae and drug doses should be independently verified with primary sources. The publisher shall not be liable for any loss, actions, claims, proceedings, demand or costs or damages whatsoever or howsoever caused arising directly or indirectly in connection with or arising out of the use of this material.

# Utilization of Contact Resistance Measurements in the Investigation of the Metallic Adhesion of Iron

T. McNICHOLES\*

*Standard Oil Company of California, Richmond, California*

AND D. V. KELLER, JR.

*Associate Professor of Metallurgy, Syracuse University, Syracuse, N. Y.*

(Received December 9, 1968)

## ABSTRACT

The utilization of contact resistance measurements in metallic systems in the presence of contaminant films has been under investigation in the electrical industry for many years. The purpose of this study was to show that the complete removal of such films could be detected by contact resistance measurements as well as the very deformation processes occurring between the asperity contact points in the interface as the contact area expands to receive the impressed load. A fully automatic apparatus was developed to record the variation of contact resistance with the applied load as an x-y plot under conditions of ultra clean or specifically contaminated metal surfaces. The samples of high purity iron (65 ppm carbon and 8 ppm carbon) were in the shape of 60 mil wires and loaded normally to 5 gms. The observed contact resistance values appeared to conform to a theoretical equation relating contact resistance and load. Room temperature creep of iron was also observed and the results agreed rather well with a proposed equation in which the contact resistance was inversely proportional to a fractional power of the applied load. A high concentration of contaminant was observed on the surface of the 65 ppm carbon iron samples which appears to be consistent with the predicted contact resistance of that system if iron carbides were in high concentration in the surface layers. Other investigators have confirmed that samples with 40 ppm carbon in iron do tend to concentrate carbon in the surficial layers.

## INTRODUCTION

FROM AN EXPERIMENTAL standpoint the investigation of the adhesion forces produced by physical contact between two metallic bodies having ideal metal-vacuum interfaces before contact reduces to an investigation of the deformation of surface asperities to accept the applied load impressed between the two bodies. As developed by Bowden and Tabor [1], Archard

[2], Greenwood and Williamson [3], and Greenwood [4], the microtopography of a metallic surface under average laboratory conditions usually consists of a multitude of asperities the shape of which is dependent on the prior history of the sample. Under the most ideal conditions, the height distribution of the asperities is usually Gaussian [4] and they appear in a rounded hill and valley contour in the size range of two microns and presumably deform during contact according to laws developed through bulk deformation analysis. The effects of surface contaminants on this deformation process have been proposed [3]; however, these have not as yet been observed experimentally even though they are intimately involved in a number of the dynamic processes, e.g. the friction process. As a consequence, it must be assumed that both clean and superficially contaminated metal systems expand the real contact area during normal loading by a similar relationship to the applied load.

The contaminant layer also acts as the only significant barrier to metallic adhesion [5, 6] which under the proper conditions can be dispersed [7]. The mechanism of contaminant film growth, for the nominally clean surface condition case is dependent upon the various energy inputs to the interface system, i.e. mechanical, thermal, etc. [7]. As a consequence of these points the experimental investigation of metallic adhesion is closely associated with the mechanical properties of the asperities during their deformation to form the real contact area and an ability to qualitatively characterize the metallic surface during this process.

## THEORY

Since the purpose of this investigation was to characterize the interface during the metallic adhesion test, a technique was established which would permit two surfaces of *known* degree of contamination to be brought into contact at a known normal load and also be capable of the detection of the fracture process while the system is unloaded. After a general survey of the possible techniques which could be used to characterize the change in the interface geometry during the adhesion cycle, e.g. constant potential, low energy electron diffraction, capacitance, thermal conductivity etc., it was evident that contact resistance was the most promising since it has been well characterized [8], the measurements are most convenient to record and the few disadvantages are characteristic of all measurements involving small contact area. The crossed-wire contact resistance technique [9] involves the passage of a very small current through one leg of each of the two crossed wires while the other legs of each are used to detect the potential drop across the interface. The observed resistance, as a consequence of its geometry, depends only on the material present at the real interface between the crossed wires.

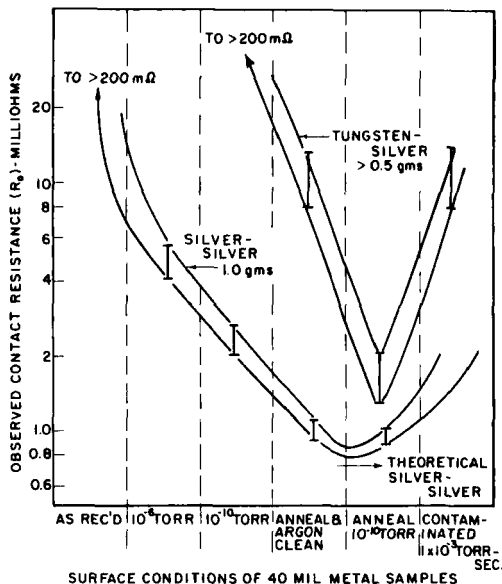


Figure 1. Contact resistance as a function of surface cleanliness for silver-silver<sup>(11)</sup> and silver-tungsten<sup>(12)</sup> couples under a one gram load.

An investigation [10] of the thermal currents generated by the passage of electrons through small contact zones has developed reasonable experimental limits such that the measurement does not alter the contact region under investigation. The sensitivity of this technique to the presence of contaminant layers is demonstrated in Figure 1 in which crossed silver [11] or silver-tungsten [12] wires (1.5 mm OD) wire loaded to a 1 gram load and the contact resistance measured under different states of surface contamination. The surfaces as represented by the conditions at the minimum in the resistance curve can be considered as being almost completely free of contaminant layers since repeated cleaning cycles, i.e. extreme argon ion bombardment and ultra high vacuum anneals ( $< 1$  nTorr), will not reduce the resistance value. A detailed discussion of the technique and the significance of these values will be presented later.

Kisluik (13) showed that the observed contact resistance ( $R_o$ ) is related to two factors

$$R_o = R_c \pm R_f \quad (1)$$

where  $R_c$  is called a constriction resistance or that due to the narrowing of the lines of the electrical field through a metallic neck region and  $R_f$  is the resistance due to that of a contaminant film or the increase in conductive path area due to tunneling effects. If only the contact resistance of an ideally clean surface system is considered,  $R_f$  may be assumed quite small; and in the first approximation, may be neglected without serious error (8).

For a single contact point the constriction resistance ( $R_c$ ) was shown by Holm (8) to be

$$R_c = \frac{\rho}{2a} \quad (2)$$

where  $\rho$  is the bulk resistivity of the metal (ohm-cm) and  $a$  is the radius of a single contact in centimeters. Recently Greenwood (14) explored the effect of multicontact points, i.e. asperity effects in the contact region, on the constriction resistance. The relationship was reported as a ratio between the area of contact as given by Holm's equation ( $A_I$ ) to that of the real area of contact ( $A_n$ ) and may be expressed approximately as

$$\frac{A_I}{A_n} = 1.4 n^{1/2} \quad (3)$$

where  $n$  is the number of contact points involved in the real contact area where  $n$  is less than 50. By substituting into Equation 3 both Holm's relationship for area ( $A_I = \pi a^2 = \pi \left(\frac{\rho}{2R_c}\right)^2$ ) and a very elementary expression (7, 8) for the increase in the real area as the load in the system is increased presuming only plastic deformation or ( $A_n = \frac{W}{3Y}$ ) where  $W$  is the impressed load and  $Y$  is the yield point of the metal involved in the contact, a relationship between contact resistance and the load is achieved

$$R_c = 1.3n^{-1/4} Y^{1/2} \rho W^{-1/2} \quad (4)$$

Equation 4 indicates that the observed contact resistance ( $R_c$ , Equation 1) between two clean metal surfaces is related to the reciprocal of the square root of the load through three variables; 1) number of contact points ( $n$ ), 2) yield point ( $Y$ ) of the material in the surficial region and 3) resistivity ( $\rho$ ) of the material in the surficial region. Let us consider each variable and its particular relationship to the loading and unloading of two ideally clean crossed-rods of about 1.5 mm diameter in a normally loaded clean adhesion experiment. In the case of silver couples and assuming all other variables constant, the effect of the number of contact points under a one gram load is illustrated in Figure 2. The variation in the number of contact points from 1 to 30 changes the contact resistance by a factor of about two which is quite negligible when compared to the effects of gross contamination. This effect appears even less consequential when one considers that at a one gram load the contact radius is only about two microns. Since the number of asperities for a metallurgically polished and etched surface of the type under consideration lies somewhere in the region of 20-30 for this area, one would suspect that the variation could be as low as 10%.

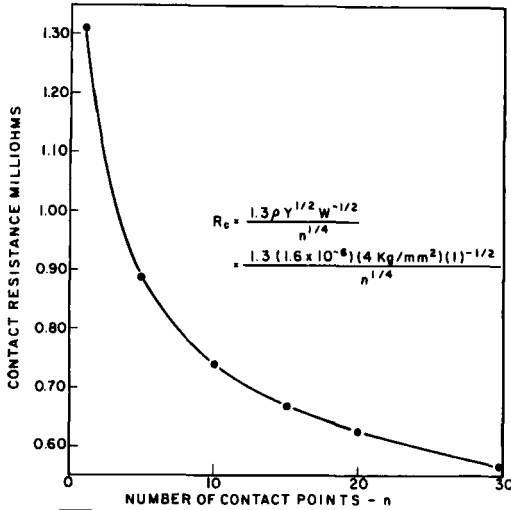


Figure 2. Variation in the contact resistance ( $R_c$ ) of silver with a variation in the number of contact points ( $n$ ) at a constant yield point and one gram load.

Iron wire samples used in this investigation were examined by metallographic techniques after exposure to many argon bombardment cleaning treatments and extreme ultra high vacuum annealing cycles usually produced an average of 20-30 asperity contacts per unit area ( $2\mu$  radius). Williamson [15] while describing the real contact area of bead blasted aluminum surfaces illustrated that, during loading the number of contact points varied with load rapidly under extremely small loads to some point at which the number of contact points remained remarkably constant as the load increased. It was submitted that as the major asperities expanded in area satellite asperities in the adjacent regions were captured (loss of one asperity point) at a rate very near to that at which new regions were brought into contact (gain one point). The value  $n$ , therefore, could be expected to increase rapidly during the very light loading stages of the contacting process and become relatively constant until gross plastic deformation consumes the entire contact region which takes place at some point above 10% compressive strain on the samples.

Figure 3 examines the effect of the assumed variation of the number of contacts ( $n$ ) on a theoretical log-log curve of contact resistance versus load for high purity iron, where the yield point was taken as  $2.5 \text{ kg/mm}^2$  (16) and the resistivity as  $9.7 \text{ micro-ohm cm}$  (17). Curve A-B assumes only one point contact as might be predicted by the Holm equation. Curve C-D assumes  $n$  increases continually with increasing load. The slope of A-B is  $-\frac{1}{2}$  as indicated by the equation; and that of C-D is slightly larger than  $-\frac{1}{2}$ . If we assume that the number of contacts is one at 0.5 g load and 30 at a 1.0

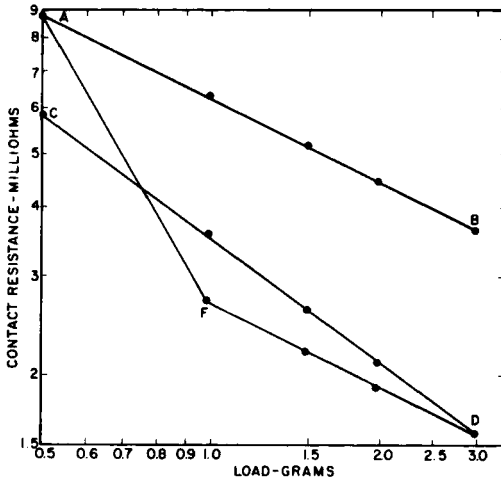


Figure 3. Theoretical curves for ultra pure iron under various condition of multi point contact of text for explanation.

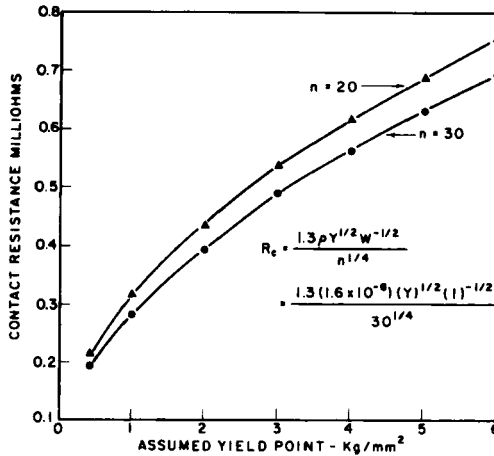


Figure 4. Variation of contact resistance ( $R_c$ ) of silver with different assumed yield points ( $Y$ ) and different number of contacts ( $n$ ) at a one gram load.

g load; and thereafter, remains constant, the curve AFD is produced. Initially a very steep slope of approximately  $-2$ ; and thereafter, a  $-1/2$  slope. Such will be considered in detail later as the most probable case.

The effect of changing the value of the yield point value for silver under a one gram load with all other variables constant is shown in Figure 4. the yield point may be increased by work hardening effects during compression and/or the absolute value of the yield point, for the metal under investigation may not be precisely known for the condition of the sample under test. In either case, the effect is not grossly significant to the overall interpretation of

one contact resistance versus loading during one cycle, i.e. loading and unloading, since each point is related to the prior point plus some small increment  $\Delta Y$  due to work hardening effects. In the overall problem of placing resistivity data on an *absolute* scale, however, this may well cause a number of problems in interpretation.

The resistivity of the metal also increases with the degree of work hardening, however, due to the low value of the resistivity change per centimeter of dislocation line ( $2 \times 10^{-10}$  ohm-cm) and the exceedingly small contact area in this system, the change would not be expected to be significant.

This point is emphasized by the examination of the contact resistance versus unloading behavior since during this phase the forces at the interface are changed causing dislocation line movements; however, excessive contact resistivity changes are not evident as will be shown later.

In conclusion, therefore, during one particular experiment as the load between two contacting metal surfaces is increased in a continuous fashion, the reactive contact resistance value would detect changes in contact radius equivalent to less than  $0.05 \mu$  provided that we make the reasonable assumption that between a load of 1.01 grams and 1.02 grams the values of resistivity yield point and the number of contact points do not change precipitously. Sufficient data has not as yet, been accumulated to relate the absolute constriction resistance to the absolute contact area. Precipitous changes in any of the variables would be readily detected as major discontinuities in observed  $R_c$  versus  $W$  curves. Such only occur at extremely light loads (0.02 gms) or under particular contaminated conditions.

## EXPERIMENTAL

Before considering the data obtained from the study of various metal systems and specific contaminants let us briefly examine the apparatus developed specifically for exploring these relationships. Generally, the apparatus is quite similar to that reported by Johnson and Keller [5, 6] except that the data taking procedure was made much more reliable by fully automating the loading process and continuously recording the variation in  $R_c$  versus  $W$  by means of an  $x-y$  recorder.

The 50 mm O.D. x 300 mm pyrex adhesion cell shown in Figure 5 was affixed to an oil pumped vacuum system through an isolation valve by means of a 40 mm pyrex-metal conflat flange which also supported side-arms for the titanium sorption pump ( $F$ ) and the argon gas supply ( $G$ ). Upon thorough degassing and partial flashing of the titanium getter immediately after bake-out, the small sorption pump maintained the adhesion cell at a pressure below 1 nTorr with the 1 inch isolation valve closed to prevent oil contamination within the cell. Several 20 cc pyrex storage cells were filled with spectrographically pure argon or contaminant gases and isolated from the ultra high



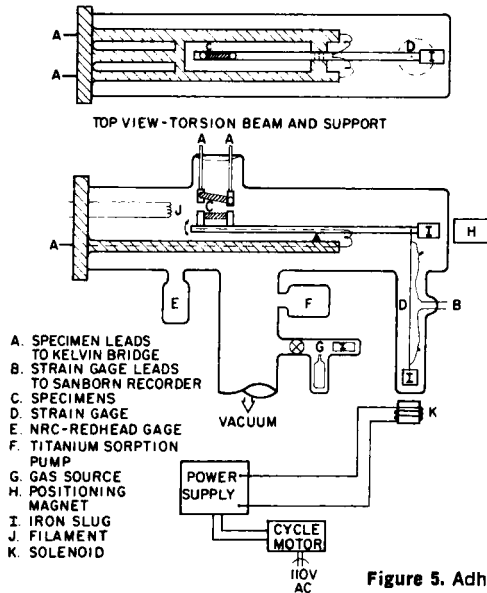


Figure 5. Adhesion cell.

vacuum (UHV) system by glass break-off seals. The gases could be metered into the system at a controlled rate. The pressure in the adhesion cell was measured by a Redhead Gage (NRC Type 752) (*E*) mounted on a 25 mm pyrex tube of low conductance in line of sight with the samples.

An alumina tube acted as a torsion balance beam and was supported by an aluminum bracket mounted on a tungsten wire at the balance point. Two 5.0 mm stainless steel support rods welded to the conflat flange supported the tungsten wire in a horizontal position. The conflat flange also supported two 12.5 mm pyrex-kovar through-seals for filament leads and power leads to the iron sample (*C*) mounted on the beam. A magnetic rod (*I*) was fixed to the torsion beam at the end opposite the sample. This magnetic rod was used to position the torsion beam relative to the fixed sample. A maximum separation of about 30 mm could be achieved between the samples for shielding during argon ion bombardment cleaning. Also fixed at the end of the beam opposite the sample was an isolated support wire for the 150 x 0.023 mm OD nude constantan strain gage wire (*D*). The lower end of the strain gage wire supported a second magnetic rod (*I*) which could interact with the field of a solenoid (*K*) outside the system and thereby move the beam sample into contact with the fixed sample. The external leads to the strain gage entered through a side-arm press-seal.

During a normal adhesion cycle (zero load to peak load to zero load) the samples were brought to a fixed separation distance of about 1 mm by adjusting the external permanent magnet (*H*) relative to the magnetic rod on the end of the torsion beam. With the beam fixed, the load was then applied to bring the samples into contact by activating the solenoid field. At

the end of the loading cycle the residual separation force was available to cause fracture, if a tensile force was necessary to fracture the junction. The load to the beam was applied by varying the line input to a DC power supply between zero and 110 volts. The power supply output was preset to a voltage corresponding to the solenoid field which was necessary to establish a desired peak contact load. The solenoid input power was then varied from zero by driving a variac with a reversible motor.

The strain gage detector consisted of a Sanborn-Model 312 transducer amplifier-indicator with the smallest division in this system corresponding to 0.02 gm. readable to within  $\pm 0.010$  grams. After each series of adhesion runs the strain gage-mass relationship was calibrated through the 0-5 gm range of operation by replacing the fixed upper sample with a calibrated force transducer. The readings of the strain gage amplifier were then compared directly to a known load. This eliminated any question of variables, such as beam flex or friction, which could arise if the system were calibrated after removal from the housing or by other indirect techniques. The range of sensitivity of the mass measurement was found to be about  $\pm 0.010g$ .

Numerous studies were made of the automatic loading profile during the standardization procedure by placing the output from the Sanborn as the input to the "y" function of an "x-y" recorder, and following the cyclic variation with time. The load was applied in a near perfect sawtooth curve with a slope of 1.42 gms/min.

The torsion beam arrangement was designed for pure normal loading in order to reduce shear forces along the interface to a minimum since small tangential movement can cause rapid dissipation of the contaminant films. The only tangential motion arose from very small but unavoidable vibrations which were only detectable under very light loads ( $< 30$  mg.) and non-adhesive conditions.

The contact resistance between the samples was monitored during the loading cycle and measured in much the same manner as previously described by Johnson and Keller [5, 6] except that the output of a Keithley Nanovolt null indicator was used as the "y" function in an x-y recorder. The x function recorded the load.

Numerous adhesion cycles were made at peak loads between 0.03 and 6.0 gms in steps of about 0.03 g for each change of surface state experienced by a sample. This technique was employed to obtain the data for Figure 1 as well as that for the other systems investigated to date, e.g. silver-silver (5, 10), silver-tungsten (11), silver-nickel (5), copper-nickel (5), titanium-titanium (6), and molybdenum-molybdenum (8).

## RESULTS AND DISCUSSION

As pointed out in the discussion of the molybdenum and titanium couples [6] and of Figure 1, the fixed load contact resistance between two samples

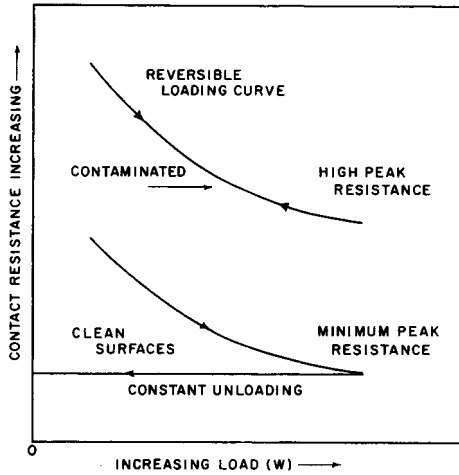


Figure 6. Characterization curves for two adhesion cycles, one contaminated, and one clean.

decreases with repeated argon ion cleaning and annealing cycles to some constant minimum resistance value. If at this point the metal surfaces consist of an ideal metal-vacuum interface, all asperity junction contacts are expected to behave in a purely metallic manner, that is compression will not grossly effect the tensile behavior of the junction. The load supporting area, therefore, is fully metallic and will not change shape until a tensile stress on the area is sufficient to initiate plastic flow and fracture [17] as shown in Figure 6. The presence of contaminants along the interface is indicated by abnormally high contact resistance values and an unloading curve which nearly superimposes on the loading curve as also shown in Figure 6. This can be explained by the existence of a plane of weakness in the interface through which a crack progresses as the load is removed and the released plastic stresses recover the shape of the interface, *cf.* discussion in [7].

Figure 7 illustrates a direct reproduction of an  $x$ - $y$  plot of an adhesion cycle obtained during the investigation of  $Fe$ - $Fe$  65 ppm carbon. Figures 8 and 9 illustrate the reproductibility of the experimental data as transferred from continuous  $x$ - $y$  recordings to log-log paper. The data points in Figures 8 and 9 were used to transfer the data which is the *only* significance of these points.

Let us examine the observed contact resistance data from Run 30 (Figure 8) for the iron couple containing 65 ppm carbon (curve  $a-d'$ ) in Figure 10 with that predicted by Equation 4 utilizing the yield strength and resistivity of pure iron and a logical variation in the number of contacts (Curve AED). Curve ( $A'F'D'$ ) represents curve ( $AFD$ ) transposed to a higher resistivity by two orders of magnitude; the apparent error in the predicted curve. Two

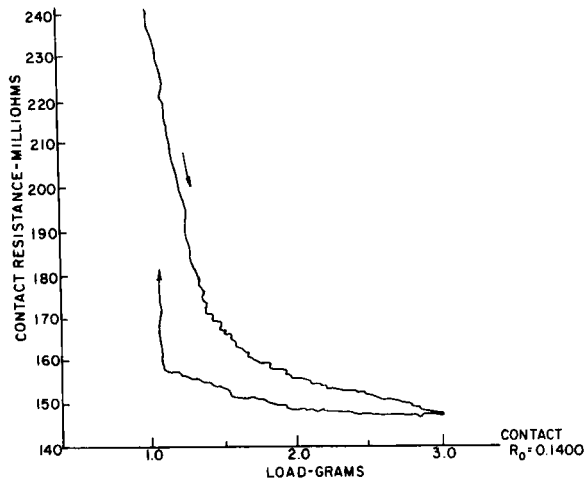


Figure 7. Typical x-y plot for iron-65 ppm carbon adhesion cycle.

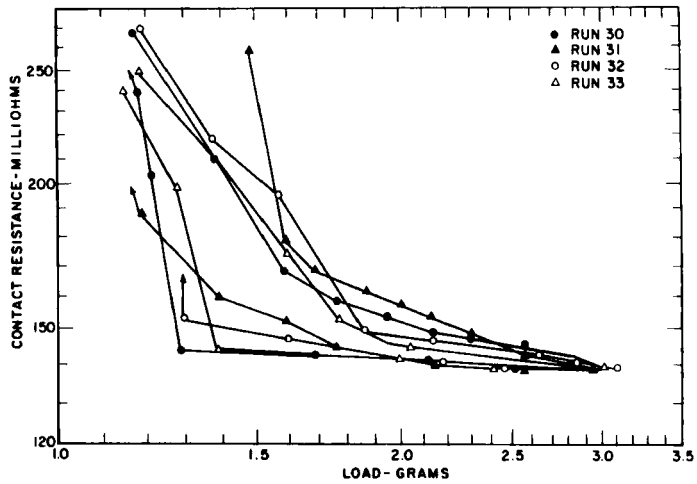


Figure 8. Several typical adhesion cycles produced from Fe-65 ppm carbon couples showing the log-log relationship.

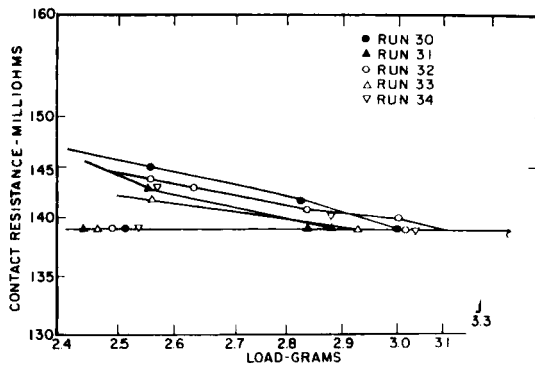


Figure 9. Expanded scale of Figure 8

of the major requisites for ultra clean iron surfaces are *not* present in the observed data at this point, i.e. the predicted resistance was not observed [5,6] or even approached and the contact area did not remain constant to the tensile region upon unloading the samples. Both of these observations were reproduced after many vigorous argon ion cleaning cycles and high temperature anneal cycles. Quite a sufficient number, as a matter of fact, to convince the observers [6], that a contaminant was present and it must have originated from within the sample. A careful examination of a recent iron-carbon equilibrium diagram [18] suggested a probable mechanism, e.g. iron carbides precipitated in the surficial layers for all concentrations of carbon in excess of at least 10 ppm at room temperature. If this were the case then the utilization of ultra pure iron resistivity and yield point values in Equation 4 would be in error since this material does not represent that in the interface. The presence of a 3-4% carbon-alloy in the interface could provide the two orders of magnitude. The resistivity of iron, for example, increases at least an order of magnitude as the carbon approaches 4% [20] and the yield point of iron could be assumed to increase sufficiently due to the carbides to account for the rest of the discrepancy. High carbon concentrations were detected by Auger electron spectra in the surface layers of Fe-40 ppm (carbon) samples which were treated in much the same manner as those described above [20].

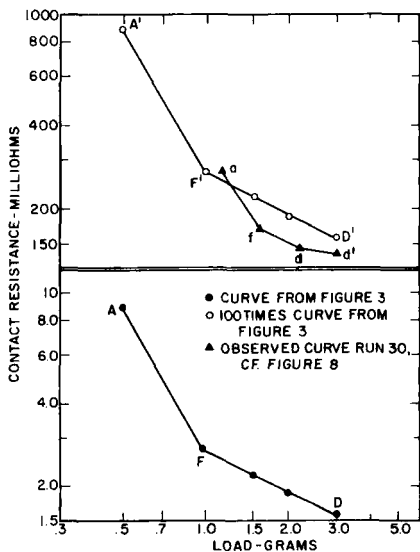


Figure 10. Comparison of the theoretical ultra pure iron curve AFD with Run 30 afdd' Curve A'F'D' is curve AFD displaced two orders of magnitude.

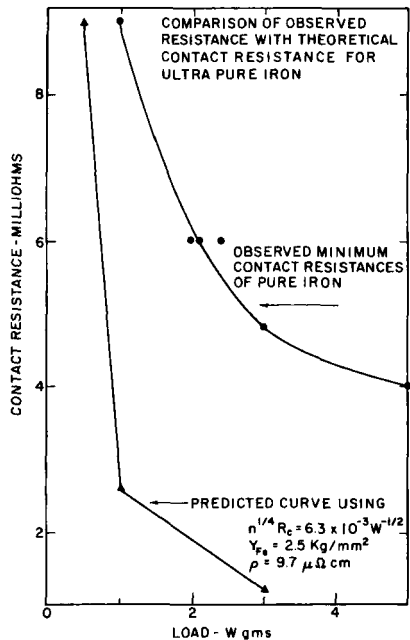


Figure 11. Comparison of the Theoretical ultra pure iron curve AFD (expanded scale) with minimum contact resistance values obtained from Fe-8 ppm carbon couples.

Dissolved oxygen or nitrogen could also cause the same adhesion phenomena. In any event, the data from run 30, etc., indicated that a surface contaminant was present and ultra pure iron was not involved.

Recently during the investigation of Fe-8 ppm carbon these observations were further substantiated as were the general predictions of contamination and contact resistance. Several data points from Fe-8 ppm carbon are compared to the theoretical AFD curve (Figure 3) of pure iron (*cf.* Figure 11). The ultra clean iron surfaces produced minimum resistances which are well within the estimations leading to Equation 4 and each case resulted in a constant contact resistance to the point of tensile failure of the junction, i.e. all of the conditions for metallic adhesion are in effect.

A number of further significant features ought to be considered in the characteristics shape of the runs 30-33 (Figure 8). The deformation process at lightloads has a slope (log-log plot) in the range of  $-2$  which changes to about  $-0.4$  as the load is increased to the range 1.6—1.7 gms. At some point greater than 2.5 gms the slope again changes to a value of  $-0.15$  or less. The degree of scatter for at least 50 separate adhesions cycles can be shown as approximately

Stage I	$-2$	$\pm 0.5$
Stage II	$-0.4$	$\pm 0.1$
Stage III	$-0.15$	$\pm 0.05$

The slope of the theoretical curve as shown in Figure 10 between A-F is approximately  $-2$  or equivalent to that of the observed data between *a-f*; furthermore, very high slopes were observed under very light loads for nearly all of the 150 runs conducted in this particular investigation. Since the change from a few asperity contacts (*A'*) to many (*F'*) was *arbitrarily* chosen as 0.5 and 1.0 gms. respectively, this could have been equally well chosen to coincide with the observed curve (*a-f*). The slope between (*f-d*) on the observed curve lies in the range  $-0.4$  which is somewhat less than that predicted in *F'D'* ( $-0.5$ ). From the previous equations and the discussion of Figure 10, it is evident that if the number of asperities in contact were increasing, the deformation slope will also increase in a continuous manner. Since the observed slope (*f-d*) is less than that calculated, i.e.  $-0.5$ , and is *linear*, the difference cannot be attributed to a continuous change in the number of contacting asperities. Since resistivity does not vary significantly with pressure, the variation between *F* and *D* might be accounted for by breakthroughs in a contaminant layer: however, such breakthroughs would abruptly decrease the contact resistance also causing non-linear increase in slope, again not in accord with that observed.

The three most likely explanations for the smaller slope seem to be:

A. That the deformation process of the asperities is an equi-mixture of

- elastic (slope  $-0.33$ ) and plastic (slope  $-0.50$ ) processes. [7].
- b. That surface creep is superimposed on the deformation curve, i.e. rate of loading sensitivity.
  - c. Surface contaminants have modified the overall deformation process.

The smallest slope ( $-0.15 \pm 0.05$ ) observed between  $d$  and  $d'$  is also a characteristic observed in Figure 10 and may signify the initiation of bulk phenomena, i.e. where the interaction between asperities is basically due to creep and bulk elastic support of the load has ensued. It is interesting to note that the slope of the creep curves mentioned below varies between  $-0.05$  and  $0.18$  depending on the work hardening of the area tested.

Although the prime purpose of these investigations were not intended to include the process of creep in the formation of the interface, preliminary studies were initiated simply by loading the samples to a fixed load and observing the variation in  $R_0$  with time. A significant amount of creep was observed in the loaded interface at room temperature, e.g.  $0.17 T_{mp}$ , between iron-iron 65 ppm carbon couples. This process corresponds to what has been described as "junction growth" of two contacting surfaces subjected to a load for a period of time [1].

The creep process also lends credence to the proposed model of rough surface contact phenomena, i.e. plastic deformation of asperities as a micro-deformation process occurring prior to the macro-elastic deformation process. Creep was not considered previously for two bodies in elastic (macro) contact since it was thought that the plasticity of the material must be involved in the creep process. We can now consider the creep process of the asperities which were plastically deformed, even though the bulk elastic point had not been exceeded.

A brief analysis of this process will illustrate the possibilities of a study of creep in a more detailed manner. Consider a relationship similar to that developed in Equation 4. If the true area ( $A_n$ ) is studied as a function of time, Tabor (21) has shown that

$$A_n = \frac{W}{P} \quad (5)$$

where  $W$  is the load and  $P$  is the yield pressure in hardness studies.

Furthermore,  $P$  is related to time ( $t$ ) by

$$P = Ct^{-1/m} \quad (6)$$

where

$$C = C_1^{-1/m} \exp(-Q/RT)^{-1/m}$$

$C_1$  = System constant

$Q$  = Activation energy of creep

$R$  = Universal constant

$T$  = Absolute temperature

$M$  = Mechanical deformation constant

by substitution

$$A_n = (W/C)t^{-1/m} \quad (7)$$

By proceeding as illustrated in the development of Equation 4 and making use of the time dependent equation for  $(C)$  we arrive at a relationship between  $R_c$  and  $t$ .

$$R_c = C_2 t^{-1/2m} \quad (8)$$

where

$$C_2 = \frac{\pi \rho^2 C_1 W}{5.6 n^{1/4}}$$

By choosing the load in the creep experiment to exceed the load (1.3 gm) where the number of contact points become constant, time becomes the only major variable in the expression. The observed slopes of numerous creep curves range from  $-0.2$  for the new contact points to  $-0.05$  for several contacts on one point. This suggests that the value of  $m$  must vary between 2.5 for the ductile deformation process and 10 for the work hardened process. These values are consistent with values suggested by Tabor.

The creep investigations were not intended to be exhaustive; and therefore, the only valid conclusion that can be drawn from the data and correlations is that a technique has been developed which shows much promise for the study of interfacial creep phenomena. The technique could also possibly develop the mechanism of contaminant layer or clean surface deformation processes, as well as the activation energy for creep in the surface layers of various states of contamination.

## CONCLUSION

In conclusion the evidence presented certainly demonstrates that a technique has been devised which aids in the characterization of surficial phenomena including deformation processes, adhesion and adhesion junction fracture. The analysis of the observed data strongly indicate that contact resistance measurements can be considered in detail in a manner relative in one adhesion cycle but a great deal of caution must be used to extrapolate these analyses to absolute values even through such an extrapolation would be most desirable. Certainly more intensive studies would supply the security necessary to make these extrapolations and provide even more details of surficial behavior. For example, the solution of the creep problem in the contact zone at zero load is generally recognized as "neck growth" in powder compacting problems and has never been examined under conditions of limited or controlled contamination. Surface diffusion is the parameter which is involved in this process. Certainly other processes will become involved as the exploration of this research area expands.



## ACKNOWLEDGEMENT

The authors would like to express their appreciation for the research support of this program by NASA.

## NOMENCLATURE

$a$	= Contact radius (One contact)
$A_I$	= Ideal area based on Holm's approximation
$A_n$	= Real contact area
$m$	= Mechanical deformation constant
$n$	= Number of asperity contact supporting the load
$p$	= Yield pressure
$Q$	= Activation energy of creep
$R$	= Universal constant
$R_o$	= Observed contact resistance
$R_c$	= Constriction resistance
$R_f$	= Film (or tunneling) resistance
$\rho$	= Resistivity of the contacting material
$T$	= Absolute temperature
$t$	= Time
$W$	= Load
$Y$	= Yield point

## REFERENCES

1. F. P. Bowden and D. Tabor, *Brit. J. Appl. Phys.* 17, (1966), p. 1521.
2. J. F. Archard, *Nature*, 172, (1951), p. 918.
3. J. A. Greenwood and J. B. P. Williamson, *Proc. Roy. Soc.*, A295, (1966), p. 300.
4. J. A. Greenwood, *J. Lub. Tech.; Trans. ASME*, 89, (1967), p. 81.
5. K. I. Johnson and D. V. Keller, Jr., *J. Appl. Phys.*, 38, (1967), p. 1896.
6. K. I. Johnson and D. V. Keller, Jr., *J. Vac. Sci. and Tech.*, 4, (1967), p. 115.
7. R. G. Aldrich and D. V. Keller, *J. Adhesion*, 1, (1969) p. 142.
8. R. Holm, "Electric Contacts," Springer-Verlag Inc., New York (1967).
9. J. J. Went, *Physica*, 8, (1941), p. 233.
10. J. B. P. Williamson, *Proc. Inst. Elect. Eng.*, 109A, (1962), p. 224.
11. D. V. Keller, Jr., "Application of Recent Static Adhesion Data to the Adhesion Theory of Friction," *Surfaces and Interfaces*, I, ed. J. Burke, V. Weiss, N. Reed, Syracuse University Press (1967), p. 225.
12. W. Saunders, Master Degree Thesis, Department of Chemical Engineering and Metallurgy, Syracuse University, Syracuse, New York (1967).
13. P. Kisluk, *Bell System Tech. J.*, 37, (1958), p. 925.
14. J. A. Greenwood, *Brit. J. Appl. Phys.*, 17, (1966), p. 1621.
15. J. B. P. Williamson, *Topography of Solid Surfaces*, presented at NASA Symposium (6) November, 1967.
16. B. Jaoul and D. Gonzales, *J. Mech. Phys. Solids*, 9, (1961), p. 16.
17. S. Arais and R. V. Colvin, *Phys. Stat. Sol.*, 6, (1964), p. 797.
18. W. Hume-Rothery, "The Structures of Alloys of Iron," Pergamon Press, New York (1966), p. 146.
19. W. E. Ruder, "Magnetically Soft Materials," *Metals Handbook*, vol. 1, 3 ed., Amer. Soc. Metals, Metals Park, Ohio, p. 786.
20. L. A. Harris, *J. Appl. Phys.*, 39, (1968), p. 1428.
21. D. Tabor, A. G. Atkins and A. Silvero, *J. Inst. Metal*, 94, (1966), p. 369.